Drag reduction in turbulent MHD pipe flows

By P. Orlandi[1]

This is a preliminary study devoted to verifying whether or not direct simulations of turbulent MHD flows in liquid metals reproduce experimental observations of drag reduction. Two different cases have been simulated by a finite difference scheme which is second order accurate in space and time. In the first case, an external azimuthal magnetic field is imposed. In this case, the magnetic field acts on the mean axial velocity and complete laminarization of the flow at $Ha = 30$ has been achieved. In the second case, an axial magnetic field is imposed which affects only fluctuating velocities, and thus the action is less efficient. This second case is more practical, but comparison between numerical and experimental results is only qualitative.

1. Introduction

Magneto-Hydro-Dynamic (MHD) flows received much attention in the sixties and, after a period of loss of interest, there is a renewal of interest shown in this activity. Attempts, for example, have been recently done in laboratory experiments (Henoch & Stace 1995) to use MHD effects as an efficient way to reduce the drag of bluff bodies in sea water. The present study is devoted to showing that some of the experimental observations in liquid metals can be qualitatively described by a coarse direct simulation of the full system of Navier-Stokes equations and magnetic field equations without any low magnetic Reynolds number approximation. For liquid metals such as sodium or mercury, the Reynolds numbers are in a range affordable by direct simulations. Direct simulation can then be used as a design tool in practical applications. In liquid metals experiments, it is almost impossible to perform flow visualizations, and measurements of turbulent quantities are complex and difficult. Direct simulations provide these desired turbulent velocity profiles.

The previous direct simulations of MHD flows were, for the major part, devoted to isotropic turbulence (Kida *et al.* 1991) and, to my knowledge, there was only one devoted to LES of flows in the presence of solid boundaries. Shimomura (1991) considered the case of a magnetic field perpendicular to the wall and, in this case, the drag increased as observed in the experiment of Reed & Likoudis (1978). On the other hand, drag reduction occurs when the magnetic field is directed in the streamwise or spanwise directions. The realization in the laboratory of the second case is easy to observe for a plane channel with a reasonable aspect ratio, but the Hartmann boundary layers on the side walls can play a role. In a circular pipe

1 Università di Roma "La Sapienza" Dipartimento di Meccanica e Aeronautica, via Eudossiana 18 00184 Roma, Italy.

one way to assign the external azimuthal magnetic field is by an electrical wire as thin as possible located at the center of the pipe; this set-up is difficult to realize and could influence the flow-field. This is why, for the case of spanwise external magnetic fields, there are a large number of experiments only for plane geometries, and some of these are listed in the review papers by Moffatt and Tsinober (1992) and by Tsinober (1990).

The realizations of an axial magnetic field inside a circular pipe is easier to set up, and two well documented experiments by Fraim & Heiser (1968) and by Krasil'nikov *et al.* (1973) are available. The friction coefficient reduction was measured at different Re and intensities of the externally applied magnetic field. The main difference between the cases of asymuthal and axial fields is that, in the case of an azimuthal field, the Lorenz force acts on the mean streamwise velocity profile, reducing the mean shear and thus the production of turbulent energy. In the presence of an axial field, the Lorenz force acts on the fluctuating components, and thus is less effective.

In both cases, without the use of superconducting materials, the efficiency, that is, the ratio between the input power and the power saved by the skin friction reduction, is very low. Thus, this approach is useful only in applications for which efficiency is not important, but it is important to reach a drag-free state. This, for example, occurs in nuclear reactors employing liquid sodium as cooling system and in some stainless steel production stages.

Dealing with liquid metals, the low magnetic Prandtl number approximation is valid. In this case, the current density can be calculated by solving one elliptic equation for the electrical potential instead of solving the full systems of Maxwell equations. This approximation was used by Shimomura (1991) and Tsinober (personal communication) in a pipe with an azimuthal external magnetic field. I made an attempt to follow this direction, but encountered numerical difficulties. Thus, I decided to solve the full system of Maxwell equations, which are straightforward to add to a code in which the Navier-Stokes equations are solved. The full solution can be used to test the solutions with the simplified equation.

2. Physical and numerical model

The dimensionless Navier-Stokes equations when a conducting fluid is subjected to a magnetic field are

$$\frac{D\mathbf{U}}{Dt} = -\nabla p + \frac{1}{Re}\nabla^2\mathbf{U} + \frac{Ha^2}{Re^2 P_m}\nabla \times \mathbf{B} \times \mathbf{B},$$

where in the Lorenz force the relationship between the current density, $\mathbf{J}$, and the magnetic field, $\mathbf{B}$, $\mathbf{J} = \nabla \times \mathbf{B}$ was used. $\mathbf{B}$ is calculated by

$$\frac{D\mathbf{B}}{Dt} = \frac{1}{Re P_m}\nabla^2\mathbf{B} + (\mathbf{B} \cdot \nabla)\mathbf{U}.$$

The dimensionless equations have been obtained by using the pipe radius R as reference length, the laminar Poiseuille velocity U_P as velocity scale, and the magnitude of the externally applied magnetic field B_0. Together with the fluid properties,

ν the kinematic viscosity, μ the magnetic permeability, and σ the electrical conductivity, the dimensionless numbers are: $Re = U_b D/\nu = U_P R/\nu$ is the Reynolds number, $P_m = \nu\mu\sigma$ is the magnetic Prandtl number, and $Ha = B_0 R\sqrt{\sigma/\rho\nu}$ is the Hartmann number.

These equations can be solved once the appropriate boundary conditions are assigned. This paper deals with flows inside a circular pipe, hence the usual no-slip conditions are assumed on the wall. Being interested only in the fully developed statistical steady state, periodicity is assumed in the streamwise direction. The components of the mean velocity **U** are $U_r = U_\theta = 0$ and $U_x(r) \neq 0$; if we assume the condition that the external magnetic field is only azimuthal, the mean magnetic field is $B_\theta = B_0 r$. On the other hand, if there is only an axial field, it must be $B_x = B_0$. By these boundary conditions, in the B_θ case, the result is that on the pipe wall there is a strong current density. In the B_x case the current density is low.

From a physical point of view it is interesting to compare the action of the Lorenz for the two cases, and the low Reynolds number approximation facilitates this analysis. With this approximation, the equations of the magnetic field are replaced by the equation for the potential of the electric field Φ which is related to the current density by $J = -\nabla\Phi + \mathbf{U} \times \mathbf{B}$. Φ can be calculated by the equation

$$\nabla^2\Phi = \nabla \cdot \mathbf{U} \times \mathbf{B},$$

which is obtained by imposing $\nabla \cdot \mathbf{J} = 0$. The components of the Lorenz force for $B_\theta = B_0 r$ are

$$\frac{\partial q_r}{\partial t} \approx \frac{Ha^2}{Re}[-\frac{r\partial\Phi}{\partial x} - q_r B_\theta]B_\theta$$

$$\frac{\partial q_x}{\partial t} \approx \frac{Ha^2}{Re}[-\frac{\partial\Phi}{\partial r} - q_x B_\theta]B_\theta$$

and for $B_x = B_0$

$$\frac{\partial q_r}{\partial t} \approx \frac{Ha^2}{Re}[-\frac{r\partial\Phi}{\partial\theta} - q_r B_x]B_x$$

$$\frac{\partial q_\theta}{\partial t} \approx \frac{Ha^2}{Re}[-\frac{r\partial\Phi}{\partial r} - q_\theta B_x]B_x.$$

The result is that in the first case the external magnetic field decreases the mean axial velocity, U_x, and thus the reduction of turbulence is more effective since the mean shear is reduced. In the second case the magnetic field acts only on the fluctuating components.

An attempt has been made to solve this simplified set of equations, but the results were not satisfactory. An initial explanation is that, to maintain a constant flow rate, the pressure gradient has to account for the part of the Lorenz force proportional to B_θ^2, and since this term at high Ha is greater than the friction losses, the evaluation of the skin friction is not accurate. Dealing with the full

system of equations, the contribution of Lorenz force to the mean pressure gradient is zero.

The second order staggered mesh finite difference scheme in space and time developed by Verzicco & Orlandi (1996) that has been tested for several laminar flows, and for rotating and non-rotating turbulent pipes (Orlandi & Fatica 1996), was adapted to solve the magnetic equations. To deal with the axis of symmetry, the quantities $h_r = rb_r, h_\theta = rb_\theta, h_x = b_x$ have been used, as was done for the velocity components ($q_r = rv_r, q_\theta = rv_\theta, q_x = v_x$). The **B** and **U** components are located at the center of the face of the cell. The fractional step method used for the velocity field was used for the magnetic field.
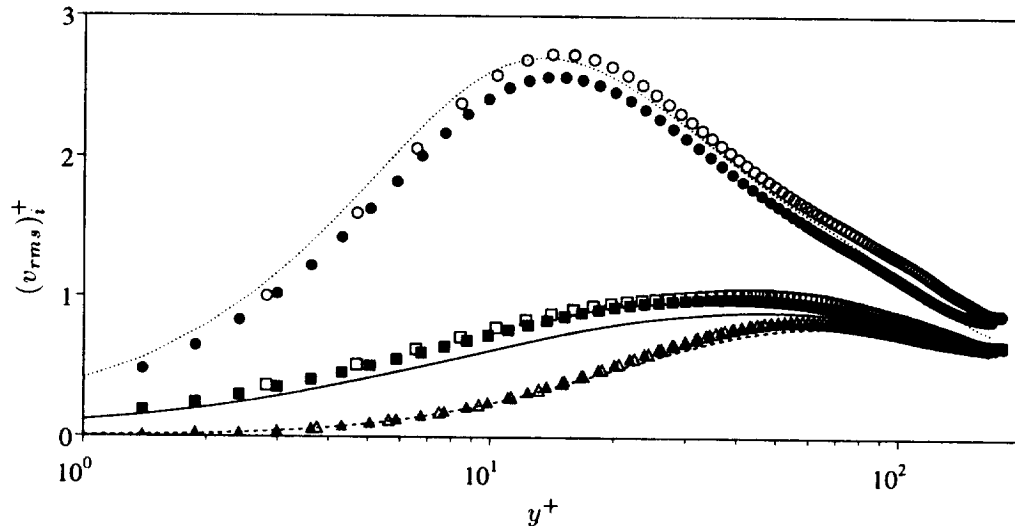

FIGURE 1.   Profiles of rms vorticity fluctuations in wall units, a) lines, present $65 \times 65 \times 65$, b) closed symbols present $129 \times 97 \times 129$ c) open symbols Eggels *et al.* $257 \times 129 \times 129$ (———— , ■, □, v'_θ), (– – – – , ▲, △, v'_r), (········ , ●, ○, v'_x).

3. Results

Without the magnetic field, the turbulence intensities are higher; therefore, the validation of the grid adequacy has been performed for $Ha = 0$. The simulation with the magnetic field requires more memory and longer CPU time because of three more parabolic equations. This study is limited to the investigation of whether or not direct simulations reproduce the drag reduction observed in the experiments. With this in mind,the strategy for the choice of the grid has been that the grid is kept as small as possible such as to give satisfactory results for the second order statistics. Fig. 1 shows that a grid with $65 \times 65 \times 65$ mesh points gives normal stresses profiles in wall units in good agreement with those by more refined simulations ($129 \times 97 \times 129$) and with that by Eggels *et al.* (1994) with a more refined grid in x. A coarse simulation does not resolve the velocity gradients, and this affects the rms profiles in a different manner. From previous simulations (Orlandi & Fatica 1996), at $Ha = 0$ it has been observed that insufficient resolution in θ and x produces a

reduction in the level of v'_r and v'_θ while that in r affects v'_x. This explains why the present coarse $v_{x,rms}$ profile near the wall agrees with that by Eggels *et al.* (1994), which was obtained by a uniform grid in r. 97 equidistant points in r located only 7 points within $y^+ = 15$, while the present nonuniform grid located 18 points in the same distance. The differences are not very pronounced, thus this resolution is satisfactory for a preliminary understanding of MHD drag reduction.
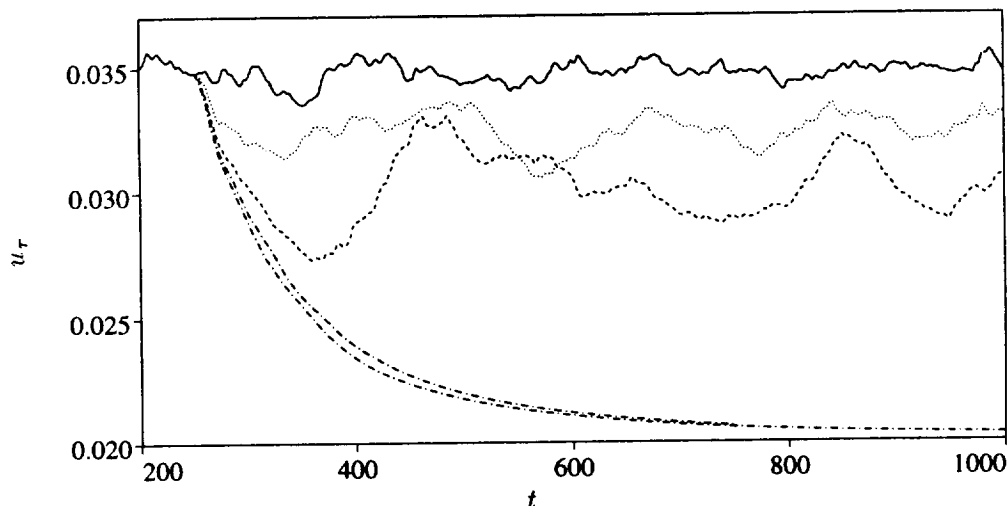

FIGURE 2. Time evolution of u_r for external B_θ (——— $Ha = 0$), (········ $Ha = 20$), (- - - - $Ha = 28$), (—·— $Ha = 30$), (—- - $Ha = 32$).

The simulations of an external azimuthal magnetic field have been performed for $Ha = 20, 28, 30$, and 32, starting from the field at $t = 250$ of $Ha = 0$ and advancing for 750 dimensionless time units. The statistics were computed from 50 fields 10 time units apart. The evolution within the first 250 time units was discarded since in this period the flow adjusts to the abrupt effects of the magnetic field. The u_r time evolution in Fig. 2 shows that this transitory period is long enough even for the high Ha number. Fig. 2 furthermore shows that the magnetic field reduces the high frequency oscillations, and that for high Hartmann numbers ($Ha \geq 30$) the flow becomes laminar. In the experiment by Branover *et al.* (1966), in a plane channel with an aspect ratio $b/a = 0.067$, the Hartman layers on the vertical wall do not play a substantial role. Thus the results could be considered for comparison with the present simulations. However also in absence of a magnetic field, the pipe and the two-dimensional channel differ, as for example shown by Durst *et al.* (1995), thus differences should be expected in the presence of the magnetic field. In the experiment $\lambda = C_{fH_a}/C_{fo}$, that is, the ratio between the C_f with and without magnetic field depends on the Reynolds number. At $Re = U_b D/\nu = 7600$ for $Ha = 20$ and 28, λ is respectively equal to 0.82 and 0.62. In the pipe it was found to be 0.86 and 0.77, and at approximately $Ha = 30$ a laminar state was achieved. Recall that, at $R_\tau = 180$ in the channel, the corresponding Reynolds number based on full width and centerline velocity is $Re = U_b 2\delta/\nu = 5600$; at this Reynolds

number the experiments of Branover *et al.* (1966) show a laminar state, and the present simulations differ more from the experiments.

The same initial conditions were used to solve the case of an axial magnetic field. Fig. 3 shows that u_r does not change considerably going from $Ha = 20$ to 60. The experiment by Fraim & Heiser for $Re = 4900$ at $Ha/Re = 0.122$ gives for the friction factor $\lambda = 0.0305$, a value smaller than 0.035 found in the present simulation. The experimental and the numerical simulations produce a value of 0.385 for $Ha = 0$. Attempts were done to perform simulations at higher Hartmann numbers to investigate whether the numerical simulation in this case also reproduces a laminar state. The numerical simulation after the initial u_r drop showed an increase of drag, associated with larger turbulent intensities near the center, and the calculation diverged. Different initial conditions such as the field for $Ha = 60$ at $t = 1000$ have also been tried without any success.
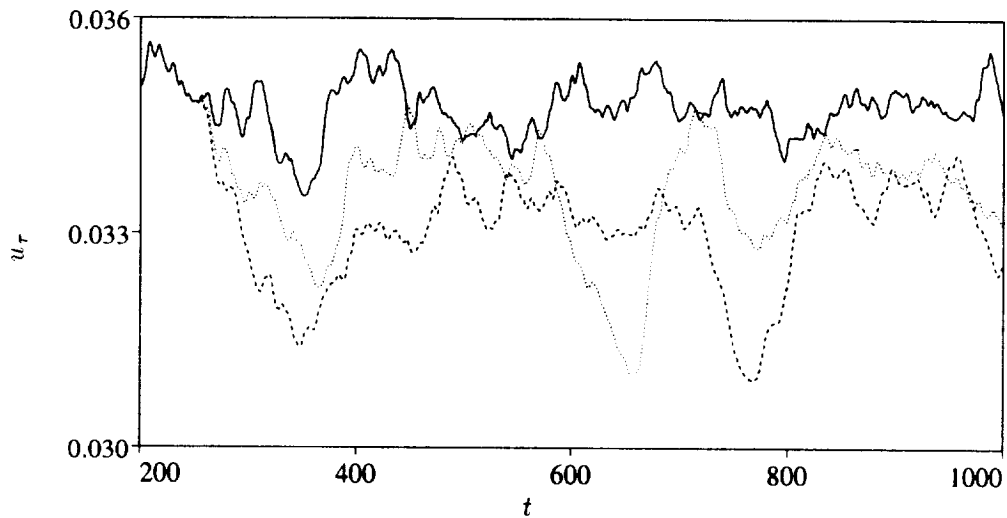

FIGURE 3. Time evolution of u_r for external B_x (——— $Ha = 0$), (······· $Ha = 20$), (– – – – $Ha = 60$).

Before discussing the velocity and *rms* velocity profiles, it is interesting to understand why in these conditions the efficiency is very low. The efficiency is defined as the ratio between the energy saved by skin friction reduction and the input energy necessary to generate the magnetic field. It is $\epsilon = (1. - \lambda)Re R_r^2 Pm^2/Ha^2$. Since for liquid metals the magnetic Prandtl number is $O(10^{-7})$, it is clear why the efficiency is very low.

In spite of these difficulties it is interesting to make a comparison between the two cases, $Ha = 28$ and $Ha = 60$. Recall that, in presence of B_θ, the Lorenz force effects the mean velocity, Fig. 4 shows that the velocity profile no longer has the *log* law and that the profile is getting close to a laminar profile. On the contrary, the case with B_x has a well defined *log* law shifted upwards, reminiscent of other flows with drag reduction.
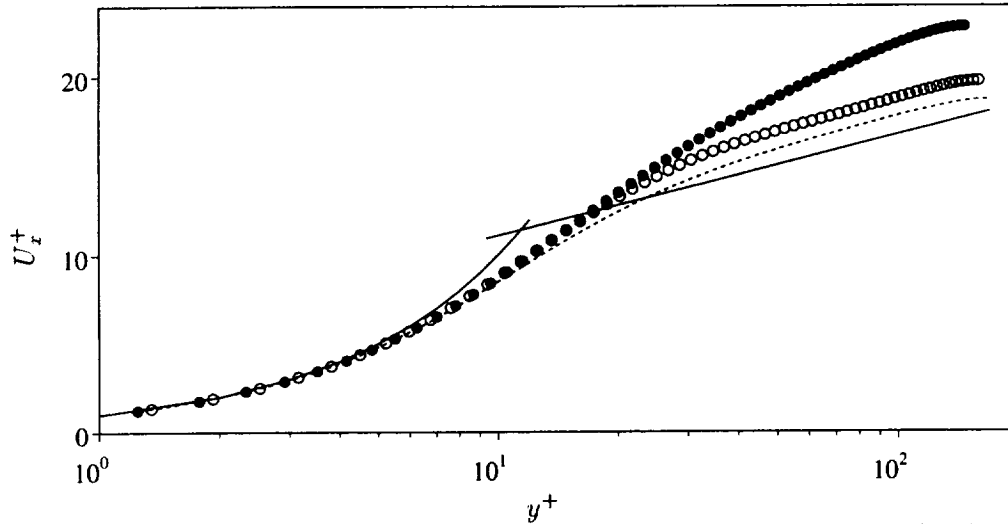
FIGURE 4.   Radial streamwise velocity profile in wall units (———— *log* law),
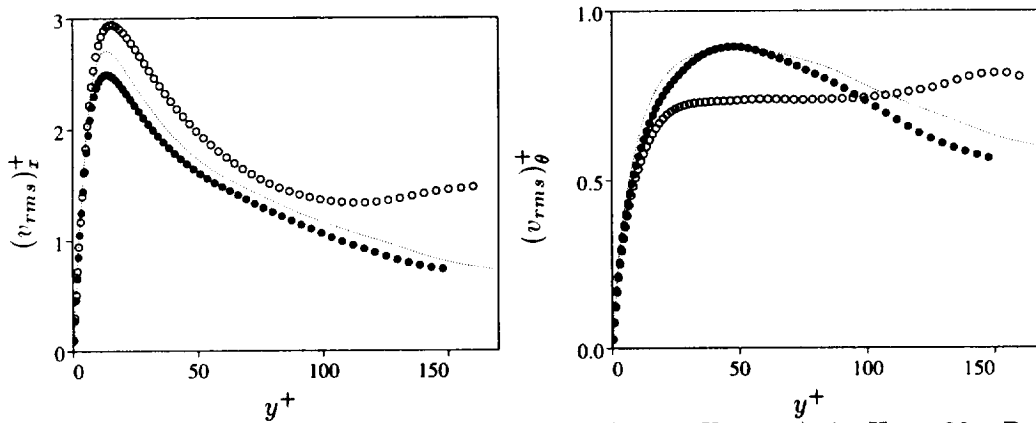(········ $Ha = 0$), (● $Ha = 28$, B_θ), (○ $Ha = 60$, B_x).

FIGURE 5.   *rms* velocity profiles in wall units (········ $Ha = 0$), (● $Ha = 28$, B_θ),
(○ $Ha = 60$, B_x).

The fields from direct simulations were used to explain through the profiles and the spectra of the normal turbulent stresses that the effects of the magnetic field are different in the two cases. The profiles of v_x' and v_r' in Figs. 5a-b show that B_θ reduces both the streamwise and the azimuthal fluctuation everywhere B_x has a more complex effect. In fact, while the axial stress increases everywhere, v_θ' is reduced in the buffer region and increases at the center. For B_θ the drag reduction is associated with a reduction of turbulent intensity. On the other hand, for B_x the reduction is associated with modifications of the vortical structures. One-dimensional azimuthal energy spectra detect the size of the energy containing eddies, which near the wall are those responsible for the wall friction. These spectra are shown for the axial and azimuthal components at $y^+ \approx 10$, the location of high turbulence production.

In discussing the spectra in Figs. 6a-b, keep in mind contour plots of fluctuating velocity even if these plots are not presented. The spectra show that B_θ reduces the energy level at the small scales and there is a transfer of energy to the large scales. The spectrum for the B_x case shows that the containing energy scale of the v_x' components are larger than those without magnetic field. These then are located at a greater distance from the wall, and thus the friction decreases. For the azimuthal stresses, B_x produces a similar transfer at the large scales, but in this case the energy level is also reduced at each wave number.
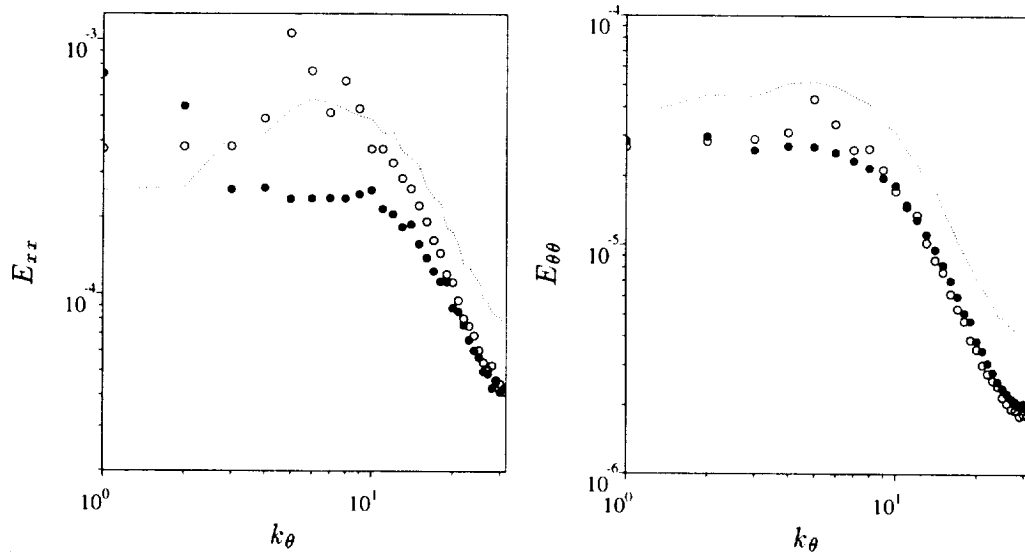

FIGURE 6.   One-dimensional energy spectra: Left: azimuthal, Right: axial directions. ($\cdots\cdots$ $Ha = 0$), ($\bullet$ $Ha = 28$, B_θ), ($\circ$ $Ha = 60$, B_x).

3. Conclusions

The present study has shown that the numerical simulation of MHD flows for liquid metal is feasible and that they can qualitatively reproduce experimental observations. It has been shown that for these fluids the drag reduction is inefficient; that is, that a large amount of electrical power must be furnished to achieve the desired goal. The reduction of the turbulent levels could be of great interest in several applications where the energy saving is not important. These direct simulations, moreover, have great interest *per se* in the study of turbulence physics when the turbulence is subjected to external forces. There are, in fact, similarities between MHD turbulence and turbulence subjected to background rotation as was claimed by Tsinober (1990). In both cases a drag reduction is achieved, but the mechanism is different. In a previous study (Orlandi 1995), it was found that background rotation breaks the symmetry of right- and left-handed vortical structures by increasing the helicity density near the wall. Thus the vortical structures have a greater degree of order leading to a reduction of production and dissipation near the wall. In the case of MHD flows the helicity density was null across the pipe

as for $Ha = 0$, and so the decrease of production and dissipation are due to the reduction of turbulence intensities. The effect is greater at the smaller scales. Thus, under the MHD effects, the small scale structures near the wall disappear and the large scales remain, producing less intense bursting events. However, the amount of disorder near the wall for MHD flows remains unchanged with respect to that of a non-rotating pipe.

It should be stressed that while these preliminary coarse direct simulations have reproduced the differences between the effects of an azimuthal and an axial magnetic field, the quantitative comparison between experimental and numeric results was poor. This needs to be explained and it requires a much longer time than that available during the summer program. All the mandatory grid resolution checks should be performed.

Acknowledgments

REFERENCES

BRANOVER, G. G., GEL'FAT, YU., M., & TSINOBER, A., 1966 Turbulent magnetohydrodynamic flows in prismatic and cylindrical ducts. *Magnetohydrodynamics.* **2**, 3-21.

DURST, F., JOVANOVIC', J. & SENDER, J. 1995 LDA measurements in the near-wall region of a turbulent pipe flow. *J. Fluid Mech.* **295**, 305-335.

KIDA, S., YANASE, S., & MIZUSHIMA, J. 1991 Statistical properties of MHD turbulence and turbulent dynamo. *Phys. Fluids A.* **3**, 457-465.

EGGELS, J. G. M., UNGER, F., WEISS, M. H., WESTERWEEL, J., ADRIAN, R. J., FRIEDRICH, R. & NIEUWSTADT, F. T. M. 1994 Fully developed turbulent pipe flow: a comparison between direct numerical simulation and experiment. *J. Fluid Mech.* **268**, 175-209.

FRAIM, F. W., & HEISER, W. H. 1968 The effect of a strong longitudinal magnetic field on the flow of mercury in a circular tube. *J. Fluid Mech.* **33**, 397-413.

HENOCH, C. & STACE, J. 1995 Experimental investigation of a salt water turbulent boundary layer modified by an apllied streamwise magnetohydrodynamic body force. *Phys. Fluids A.* **7**, 1371-1383.

KRASIL'NIKOV, E., YU, LUSHCHICK, V. G., NIKOLAENKO, V. S. & PANEVIN, I. G. 1970 Experimental study of the flow of an electrically conducting liquid in a circular tube in an axial magnetic field. *Fluid Dynamics.* **6**, 317-320.

MOFFATT, H. K. & TSINOBER, A. 1992 Helicity in laminar and turbulent flow. *Annu. Rev. Fluid. Mech.* **24**, 281-312.

ORLANDI, P. 1995 Helicity fluctuations and turbulent energy production in rotating and non-rotating pipes. *Annual Research Brief of CTR*, Center for Turbulence Research, NASA Ames/Stanford Univ., 198-208.

ORLANDI, P. & FATICA, M. 1996 Direct simulations of a turbulent pipe rotating along the axis. In the review process for *J. Fluid Mech.*

REED, C. B. & LIKOUDIS, P. S. 1978 The effect of a transverse magnetic field on shear turbulence. *J. Fluid Mech.* **89**, 147-171.

SHIMOMURA, Y. 1991 Large eddy simulation of magnetohydrodynamic turbulent channel flows under a uniform magnetic field. *Phys. Fluids A.* **3**, 3098-3106.

TSINOBER, A. 1990 MHD flow drag reduction. *Viscous drag reduction in boundary layers* Edited by D. M. Bushnell & J. N. Hefner Progress in Astronautics and Aeronautics. **123**, 327-349.

TSINOBER, A., 1990 Turbulent Drag Reduction Versus Structure of Turbulence. *Structure of Turbulence and Drag Reduction.* Ed. A. Gyr. Berlin: Springer Verlag. 313-340.

VERZICCO, R. & ORLANDI, P. 1996 A finite difference scheme for direct simulation in cylindrical coordinates. *J. Comp. Phys.* **123**, 402-414.